Semiconductor Physics, Quantum Electronics & Optoelectronics, 2014. V. 17, N 3. P. 232-236.

PACS 78.40.Ha, 77.80.Bh

Structural and optical studies of $(Ag_3AsS_3)_{0.6}(As_2S_3)_{0.4}$ thin films deposited at different technological conditions

I.P. Studenyak[1], Yu.Yu. Neimet[1], Y.Y. Rati[1], M.Yu. Buchuk[1], S. Kökényesi[2], L. Daróci[2], R. Bohdan[2]
[1]*Uzhhorod National University, Faculty of Physics,*
3, Narodna Sq., 88000 Uzhhorod, Ukraine
[2]*University of Debrecen, Department of Experimental Physics, Faculty of Science and Technology,*
18/a Bem Sq., 4026 Debrecen, Hungary,
E-mail: studenyak@dr.com

Abstract. $(Ag_3AsS_3)_{0.6}(As_2S_3)_{0.4}$ thin films were deposited upon a quartz substrate by rapid thermal evaporation at temperatures 1050, 1200, and 1350 °C. Structural studies of the as-deposited thin films were carried out by scanning electron microscopy and atomic force microscopy. It is shown that the surfaces of all the films were covered with Ag-rich crystalline micrometer sized cones. The optical transmission spectra for as-deposited thin films were studied at room temperature. The absorption spectra in the region of its exponential behaviour were analyzed, the dispersion dependences of refractive index as well as their variation depending on evaporation temperature were investigated.

Keywords: thin film, thermal evaporation, SEM, AFM, optical absorption.

Manuscript received 26.02.14; revised version received 24.07.14; accepted for publication 16.09.14; published online 30.09.14.

1. Introduction

Chalcogenide glasses have been extensively studied in the last several decades. They have shown numerous applications in various areas of science and technology. High photosensitivity of some chalcogenides was used to obtain materials for optical recording [1]. Surface patterns were recorded on the As_2S_3 film doped with silver [2]. Photo-induced effects have been studied in a rather big part of the papers, involving relatively impressive number of researches. It should be noted that some of such papers were reviewed in Ref. [3]. Chalcogenides doped with metals demonstrate also interesting electrical properties. Thus, silver ion movements that arise due to electrical voltage inside a chalcogenide amorphous matrix base have been utilized in creation of solid state ionic memory elements [4]. Mass transport, observed in chalcogenide thin films and driven by the electrochemical processes, can be used in solid state electronics and integrated optics with the same success [5].

Different experimental methods have been used up to date to deposite thin films with a high quality of a bulk structure and a surface. The methods themselves can strongly influence the structure, surface, and physics properties of prepared thin films. Among silver-containing chalcogenides the thin films of Ag-As-S ternary system have a remarkable place. Thin films in this system, as in many other similar ones, were mostly prepared by a deposition onto the substrates by using vacuum coating techniques, i.e. thermal evaporation, accompanied by a thermally or photo-induced dissolution of silver in As_2S_3 matrix [6, 7] or pulse laser deposition (PLD) [8]. A rather new method used is spin-coating technique [9, 10]. By the means of the PLD technique a potentiometric thin film sensor can be realized on the basis of chalcogenide glasses (in particular Ag-As-S) [11].

Recently, we have reported about structure [12], electrical conductivity [13], and optical absorption [14] in superionic Ag_3AsS_3–As_2S_3 glasses and composites. In this paper, we study the deposition technology of $(Ag_3AsS_3)_{0.6}(As_2S_3)_{0.4}$ thin films and influence of the evaporation temperature on its structural and optical properties which includes scanning electron microscopy (SEM) and atomic force microscopy (AFM) as well as the spectroscopic investigations of transmission and absorption spectra, refractive indices and their dispersion curves due to the change of evaporation temperature.

2. Experimental

Synthesis of $(Ag_3AsS_3)_{0.6}(As_2S_3)_{0.4}$ composite material (that consists of crystalline Ag_3AsS_3 and glassy As_2S_3 [13]) was carried out at a temperature of 700 °C for 24 h with subsequent melt homogenization for 72 h. $(Ag_3AsS_3)_{0.6}(As_2S_3)_{0.4}$ thin films were prepared by rapid thermal evaporation from the corresponding composite material at temperatures 1050, 1200 and 1350 °C in vacuum ($3\cdot10^{-3}$ Pa) by using a VU-2M setup. The composite material was initially placed in a tantalum evaporator, perforated for preventing the material falling out, on a glass substrate kept at room temperature. The film thickness was measured using an Ambios XP-1 profile meter. Structural properties of the thin films under investigation were studied using SEM (Hitachi S-4300) and AFM (Nanoscope 3100). Energy-dispersive X-ray spectroscopy (EDX) was used to ensure the thin film chemical composition. Optical transmission spectra of the thin films were studied at room temperature by using the MDR-3 grating monochromator. Based on the interference transmission spectra, the spectral dependences of optical absorption coefficient as well as refractive index dispersion dependences were obtained [15].

3. Results and discussion

SEM and AFM images that characterize the surface of $(Ag_3AsS_3)_{0.6}(As_2S_3)_{0.4}$ thin films are given in Figs 1 and 2. It is shown the presence of cones on the top of a freshly evaporated thin film surface, which remind the whiskers, discovered rather long ago [16]. The number of cones increases with evaporation temperature increase and the average density of the cones at the surface of the thin film deposited at evaporation temperature 1350 °C equals approximately 14×10^3 per mm^2. The average height of the cones is found to be 2.5 μm which is well seen from the AFM image in Fig. 2c, and it is also confirmed by the profile meter. As estimated by the profile meter, the thicknesses of the base film layer are listed in Table. Meanwhile, the average base diameter of the cones is about 2 μm. This value is in good agreement with the detailed SEM study of the film under investigation. The average aspect ratio (height over diameter) of the cones was estimated and found to be 1.2.

EDX technique enabled us to ensure the composition of thin films, deposited at different evaporation temperatures. It is shown that at the evaporation temperature 1050 °C thin film contains less amount of Ag (nearly 5 times), greater amount of As (more than 2 times) and approximately the same amount of S in comparison with initial material of composite (Table). With evaporation temperature increase to 1200 °C, the content of Ag slightly grows whereas the content of S slightly decreases. The most close to Ag content is composition of thin film deposited at 1350 °C since it is As-enriched and has a deficiency of sulphur

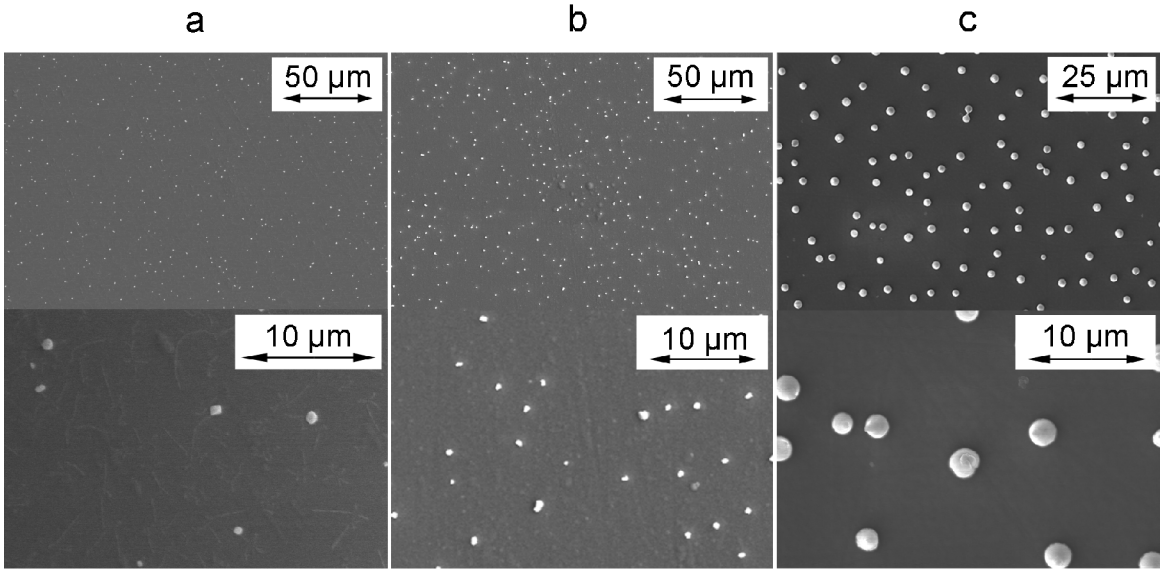

Fig. 1. SEM images of $(Ag_3AsS_3)_{0.6}(As_2S_3)_{0.4}$ thin films evaporated at temperatures (a) 1050 °C, (b) 1200 °C, and (c) 1350 °C.

percentage in comparison with the initial bulk composite, as follows in Table. Simultaneously, the local EDX analysis estimated an excess of silver in the atomic composition of the cones (62.8%). The presence of small amounts of arsenic (18%) and sulphur (19.2%) in the cones shown by the EDX can be explained by the fact that the minimum estimation area covers not only the cone itself, but some part of the base film as well. An excess of silver in the EDX results on cones enable us to ascribe the cones, observed in $(Ag_3AsS_3)_{0.6}(As_2S_3)_{0.4}$ thin film, to silver crystals or crystalline Ag-rich structures.

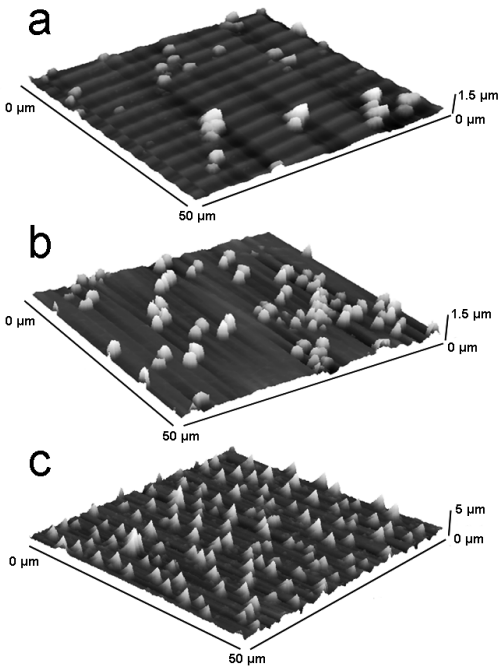

Fig. 2. AFM images of $(Ag_3AsS_3)_{0.6}(As_2S_3)_{0.4}$ thin films evaporated at temperatures (a) 1050 °C, (b) 1200 °C, and (c) 1350 °C with recorded holographic patterns.

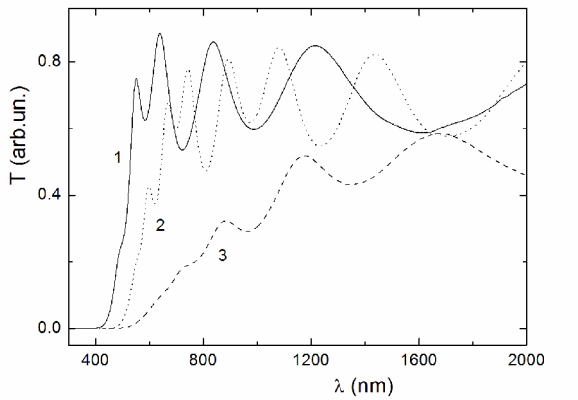

Fig. 3. Optical transmission spectra of $(Ag_3AsS_3)_{0.6}(As_2S_3)_{0.4}$ thin films evaporated at temperatures (1) 1050 °C, (2) 1200 °C, and (3) 1350 °C.

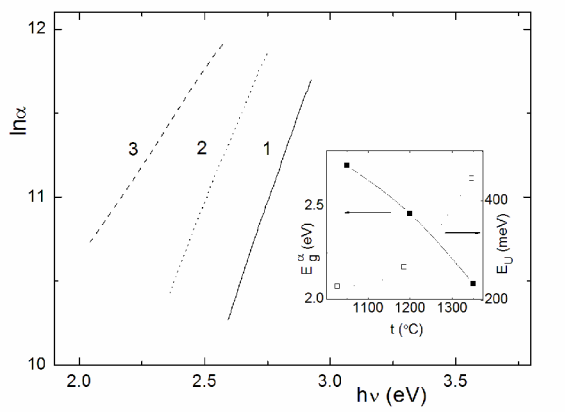

Fig. 4. Absorption edge spectra of $(Ag_3AsS_3)_{0.6}(As_2S_3)_{0.4}$ thin films evaporated at temperatures (1) 1050 °C, (2) 1200 °C, and (3) 1350 °C. The inset shows the dependences of energy position of absorption edge (1) and the Urbach energy (2) on the temperature of evaporation.

Fig. 3 shows the optical transmission spectra of $(Ag_3AsS_3)_{0.6}(As_2S_3)_{0.4}$ thin films deposited at temperatures 1050, 1200 and 1350 °C. One can observe decrease of transmission by almost 20% as well as the transmission onset shifts towards longer wavelengths with evaporation temperature increase. Besides, with evaporation temperature increase the spectra of the as-deposited films at the onset of transmission are seen to be more smeared. This fact is characteristic for a structural disordering that occurs in the film structure as a consequence of evaporation temperature increase. Fig. 4 presents the absorption edge spectra of the as-deposited $(Ag_3AsS_3)_{0.6}(As_2S_3)_{0.4}$ thin films in the range of their exponential behaviour. It should be noted that two spectral regions can be taken into consideration in amorphous films at the fundamental absorption edge at high absorption levels – the Tauc region and exponential one [17]. In this case, both the Tauc gap E_g^{opt} and the energy position of the exponential absorption edge E_g^{α} at a fixed absorption coefficient α (for example, in Ref. [18] the α value was chosen to be $\alpha = 10^4$ cm^{-1}), characterizing the exponential part of the absorption edge, were used. In our case we used the E_g^{α} values taken at $\alpha = 5 \cdot 10^4$ cm^{-1} for the characterization of the absorption edge spectral position. Determined in such a way E_g^{α} values are presented in Table, where the E_g^{opt} values calculated for the Tauc region are listed for comparison as well. It is shown that with evaporation temperature increase from 1050 to1350 °C the value of E_g^{α} decreases by 0.628 eV and for thin film deposited at temperature 1350 °C it is equal 2.085 eV (Table).

It is seen from Fig. 4 that the optical absorption edge spectra in the range of their exponential behaviour in the thin films under investigation can be fitted by Eq. [19]

Table. Structural and optical parameters of $(Ag_3AsS_3)_{0.6}(As_2S_3)_{0.4}$ thin films evaporated at temperatures 1050, 1200, and 1350 °C.

Thin film No.	Evaporation temperature, °C	Composition, at.%			Thickness (nm)	n (1.5 μm)	E_g^{α} (eV) at $\alpha = 5\cdot10^4\,\mathrm{cm}^{-1}$	E_g^{opt} (eV)	E_U (meV)
		Ag	As	S					
		Initial							
		29.0	22.6	48.4					
1	1050	5.7	46.5	47.8	480	2.472	2.713	2.258	228
2	1200	8.4	47.5	44.2	690	2.658	2.459	1.996	267
3	1350	29.0	32.0	39.0	500	3.085	2.085	1.708	457

$$\alpha(h\nu,T) = \alpha_0 \cdot \exp\left[\frac{h\nu - E_0}{E_U}\right], \quad (1)$$

where E_U is the Urbach energy (a reciprocal of the absorption edge slope $E_U^{-1} = \Delta(\ln\alpha)/\Delta(h\nu)$), α_0 and E_0 are the convergence point coordinates of the Urbach bundle. It should be noted that the Urbach energy E_U characterizes the smearing of optical absorption edge (in fact the E_U is a degree of the system disordering). It was shown in Ref. [20] that both temperature and structural disordering affect the absorption edge shape in amorphous materials, i.e. the Urbach energy E_U is described by equation

$$E_U = (E_U)_T + (E_U)_X, \quad (2)$$

where $(E_U)_T$ and $(E_U)_X$ are the contributions of temperature disordering and structural disordering to E_U, respectively. The temperature disordering arises due to the thermal vibrations of atoms and structural elements. The structural disordering in amorphous materials is related to the absence of long-range order, the presence of structural inhomogeneities, i.e. defects, pores, etc. It should be noted that with evaporation temperature increase from 1050 to1350 °C the value of E_U increases by 229 meV and for thin film deposited at temperature 1350 °C it is equal 457 meV (Table). The highest value of E_U and correspondingly the highest degree of structural disordering for the thin film deposited at 1350 °C are caused by the presence of high amounts of such structural defects as the cones on their surface.

The dispersion dependences of the refractive index for the as-deposited thin films were obtained from the interference transmission spectra (Fig. 5). The slight dispersion of the refractive index is observed in the transparency region while it increases when approaching to the optical absorption edge region. It is shown that with evaporation temperature increase from 1050 to1350 °C the refractive index increases by 24.8% and for thin film deposited at temperature 1350 °C it is equal 3.085 (Table).

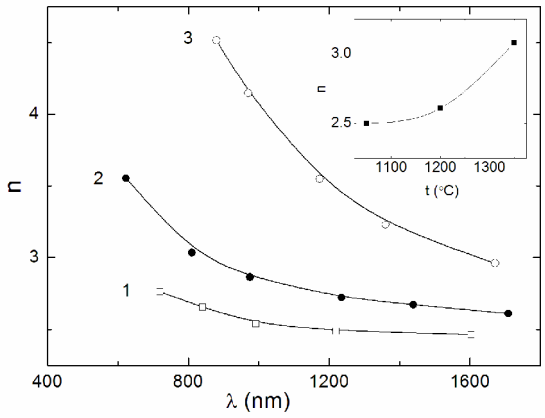

Fig. 5. Refractive indices dispersions of $(Ag_3AsS_3)_{0.6}(As_2S_3)_{0.4}$ thin films evaporated at temperatures (1) 1050 °C, (2) 1200 °C, and (3) 1350 °C. The inset shows the refractive indices dependence on the temperature of evaporation.

4. Conclusions

$(Ag_3AsS_3)_{0.6}(As_2S_3)_{0.4}$ thin films were prepared using the rapid thermal evaporation at temperatures 1050, 1200 and 1350 °C. SEM and AFM imaging of the thin films revealed numerous micrometer-sized cones on their surfaces, number of which increased with evaporation temperature grow. The EDX analysis showed an excess of silver in the obtained cones, which enabled us to ascribe the last one to the cones. The composition of thin film deposited at 1350 °C has Ag content most close to initial bulk since it is As-enriched and have a deficiency of sulphur.

The optical transmission spectra of thin films have shown the decrease of transmission by almost 20%, the transmission onset shifts towards longer wavelengths and smeared with evaporation temperature increase. The spectral dependences of the absorption coefficient as well as dispersion dependences of the refractive index were derived from the spectrometric studies of interference transmission spectra. In the range of the exponential behaviour of the optical absorption edge, the energy position of exponential absorption edge E_g^{α} and Urbach energy E_U in $(Ag_3AsS_3)_{0.6}(As_2S_3)_{0.4}$ thin films

were determined. It was shown that the evaporation temperature increase leads to the decrease of E_g^{α}, increase of E_U and increase of the refractive index n.

Acknowledgements

The authors are grateful to the TAMOP Grant (TAMOP 4.2.2.A-11/1/KONV-2012-0036 project) which is co-financed by the European Union and European Social Fund. Yuriy Neimet (contract number 51301014) is strongly grateful to the International Visegrad Fund scholarship for the funding of the project.

References

1. T. Ohta, Phase-change optical memory promotes the DVD optical disc // *J. Opt. Adv. Mat.* **3**, p. 609-626 (2001).
2. R.E. Belford, E. Hajto, A.E. Owen, The selective removal of the negative high-resolution photoresist system Ag-As-S // *Thin Solid Films*, **173**, p. 129-137 (1989).
3. M. Frumar, Z. Cernosek, J. Jedelsky, B. Frumarova, T. Wagner, Photoinduced changes of structure and properties of amorphous binary and ternary chalcogenides // *J. Opt. Adv. Mat.* **3**(2), p. 177-188 (2001).
4. M.N. Kozicki, M. Mitkova, M. Park, M. Balakrishnan, G. Gopalan, Information storage using nanoscale electrodeposition of metal in solid electrolytes // *Superlattices and Microstructures*, **34**, p. 459-465 (2003).
5. M.N. Kozicki, M. Mitkova, Mass transport in chalcogenide electrolyte films – materials and applications // *J. Non-Cryst. Solids*, **352**, p. 567-577 (2006).
6. T. Wagner, V. Perina, A. Mackov, E. Rauhala, A. Seppala, Mir. Vlcek, S.O. Kasap, Mil. Vlcek, M. Frumar, The tailoring of the composition of Ag–As–S amorphous films using photo-induced solid state reaction between Ag and $As_{30}S_{70}$ films // *Solid State Ionics*, **141–142**, p. 387-395 (2001).
7. A. Kovalskiy, H. Jain, M. Mitkova, Evolution of chemical structure during silver photodiffusion into chalcogenide glass thin films // *J. Non-Cryst. Solids*, **355**, p. 1924-1929 (2009).
8. P. Nemec, M. Frumar, J. Jedelsky, M. Jelınek, J. Lancok, I. Gregora, Thin amorphous chalcogenide films prepared by pulsed laser deposition // *J. Non-Cryst. Solids*, **299-302**, p. 1013-1017 (2002).
9. T. Wagner, T. Kohoutek, Mir. Vlcek, Mil. Vlcek, M. Munzar, M. Frumar, Spin-coated $Ag_x(As_{0.33}S_{0.67})_{100-x}$ films: preparation and structure // *J. Non-Cryst. Solids*, **326-327**, p. 165-169 (2003).
10. T. Kohoutek, T. Wagner, J. Orava, M. Frumar, V. Perina, A. Mackova, V. Hnatowitz, M. Vlcek, S. Kasap, Amorphous films of Ag–As–S system prepared by spin-coating technique, preparation techniques and films physico-chemical properties // *Vacuum*, **76**, p. 191-194 (2004).
11. M.J. Schoening, C. Schmidt, J. Schubert, W. Zander, S. Mesters, P. Kordos, H. Lueth, A. Legin, B. Seleznev, Yu.G. Vlasov, Thin films on the basis of chalcogenide glass materials prepared by pulsed laser deposition technique // *Sensors and Actuators B*, **68**, p. 254-259 (2000).
12. I. Studenyak, Yu. Neimet, C. Cserhati, S. Kökényesi, E. Kazakevičius, T. Šalkus, A. Kežionis, A. Orliukas, Structural and electrical investigations of $(Ag_3AsS_3)_x(As_2S_3)_{1-x}$ superionic glasses // *Cent. Eur. J. Phys.* **10**, p. 206-209 (2012).
13. I.P. Studenyak, Yu.Yu. Neimet, M. Kranjčec, A.M. Solomon, A.F. Orliukas, A. Kežionis, E. Kazakevičius, T. Šalkus, Electrical conductivity studies in $(Ag_3AsS_3)_x(As_2S_3)_{1-x}$ superionic glasses and composites // *J. Appl. Phys.* **115**, 033702-1−033702-5 (2014).
14. I.P. Studenyak, M. Kranjcec, Yu.Yu. Neimet, M.M. Pop, Optical absorption edge in $(Ag_3AsS_3)_x(As_2S_3)_{1-x}$ superionic glasses // *Semiconductor Physics, Quantum Electronics & Optoelectronics*, **15**(2), p. 147-151 (2012).
15. R. Swanepoel, Determination of the thickness and optical constants of amorphous silicon // *J. Phys. E: Sci. Instrum*. **16**, p. 1214-1222 (1983).
16. R.S. Wagner, W.C. Ellis, Vapour-liquid-solid mechanism of single crystal growth // *Appl. Phys. Lett.* **4**, p. 89-90 (1964).
17. R. Bindemann, O. Paetzold, The influence of thermal disorder on the absorption edge in the Tauc region of a–Si:H // *Phys. Status Solidi* (*b*), **160**, p. K183-K188 (1990).
18. S. Kökényesi, J. Csikai, P. Raics, I.A. Szabo, S. Szegedi, A. Vitez, Comparison of photo- and deuteron-induced effects in amorphous chalcogenide layers // *J. Non-Cryst. Solids*, **326-327**, p. 209-214 (2003).
19. F. Urbach, The long-wavelength edge of photographic sensitivity and of the electronic absorption of solids // *Phys. Rev.* **92**, p. 1324-1326 (1953).
20. G.D. Cody, T. Tiedje, B. Abeles, B. Brooks, Y. Goldstein, Disorder and the optical-absorption edge of hydrogenated amorphous silicon // *Phys. Rev. Lett.* **47**, p. 1480-1483 (1981).